Computing Symmetry Sets from 3D Shapes

Arjan Kuijper

IT University Technical Report Series **TR-2004-48**

ISSN 1600–6100 **September 2004**

ISSN 1600–6100

ISBN87-7949-070-0

Copies may be obtained by contacting:

IT University of Copenhagen
Rued Langgaards Vej 7
DK-2300 Copenhagen S
Denmark

Telephone: **+45 72 18 50 00**
Telefax: **+45 72 18 50 01**
Web `www.itu.dk`

Contents

Abstract

In this paper we discuss the implementation of 3D Symmetry Sets. It describes how the Symmetry Set can be derived given a parametrized shape, as well as given an unorganized point cloud. It presents a geometric method to derive the Symmetry Set, that is an extension of the one given in deliverable 10. Just as in the 2D case, level set methods cannot be applied. Although the mathematics are a simple extension of the 2D case, the visualization, numerical computations and their stability are complicated. An example is give by means of a ellipsoid. In this example the Symmetry Set can be computed exactly and results can be compared to the ground truth.

1 General theory on shapes in 3D

In this work we consider shapes in 3D. These shapes are considered to be closed 2D manifolds that allow a parameterization for the purpose of computing the Symmetry Set by the standard defintion introduced by Bruce, Giblin and Gibson [1].

1.1 Curvatures

Let $L(x, y, z) = 0$ define implicitly a shape. Then its Gaussian surface curvature K and Mean surface curvature H (Koenderink, [6], p. 515) are given by

$$\begin{aligned} K &= \frac{L_x^2 L_{yy} L_{zz} + L_y^2 L_{xx} L_{zz} + L_z^2 L_{xx} L_{yy}}{(L_x^2 + L_y^2 + L_z^2)^2} \\ H &= \frac{L_x^2(L_{yy} + L_{zz}) + L_y^2(L_{xx} + L_{zz}) + L_z^2(L_{xx} + L_{yy})}{2(L_x^2 + L_y^2 + L_z^2)^{\frac{3}{2}}} \end{aligned}$$

and the minimal and maximal curvatures follow from

$$\begin{aligned} \kappa_{max} &= H + \sqrt{H^2 - K} \\ \kappa_{min} &= H - \sqrt{H^2 - K} \end{aligned}$$

1.2 Umbilic points

At umbilic points (Porteous, [12] , p. 267) the two prinipal curvatures coincide and $H^2 = K$.These points are generically isolated points. Also both evolutes intersect at these points. All other intersections of the two evolutes are due to different points of the shape.

1.3 Ridge liness

On the shape ridges can be identified, defined as those points with locally extremal curvature in one direction.

1.4 Evolutes

Since there are two distince curvatures, we can assign to each point the points $\mathcal{S} + \mathcal{N}/\kappa_{min}$ and $\mathcal{S} + \mathcal{N}/\kappa_{max}$. They define two evolutes, representing the maximal and the minimal curvatures.

1.5 The Medial Axis in 3D

Although there has been no publication on 3D Symmetry Sets (yet), there has been published quite a lot of work on deriving and presenting the Medial Axis in 3D. Most of the geometrical approaches that incorporate knowledge of possible and allowed transitions is due to Leymarie proposing a method to derive the Medial Axis in 3D [8, 9, 7, 10, 11], as well as Kimia and Giblin, who give a formal classification of the Medial Axis points [2, 4] and transitions [3] Also Voronoi diagrams to detect the skeleton, in combination with ridges for additional information, has been reported [5].

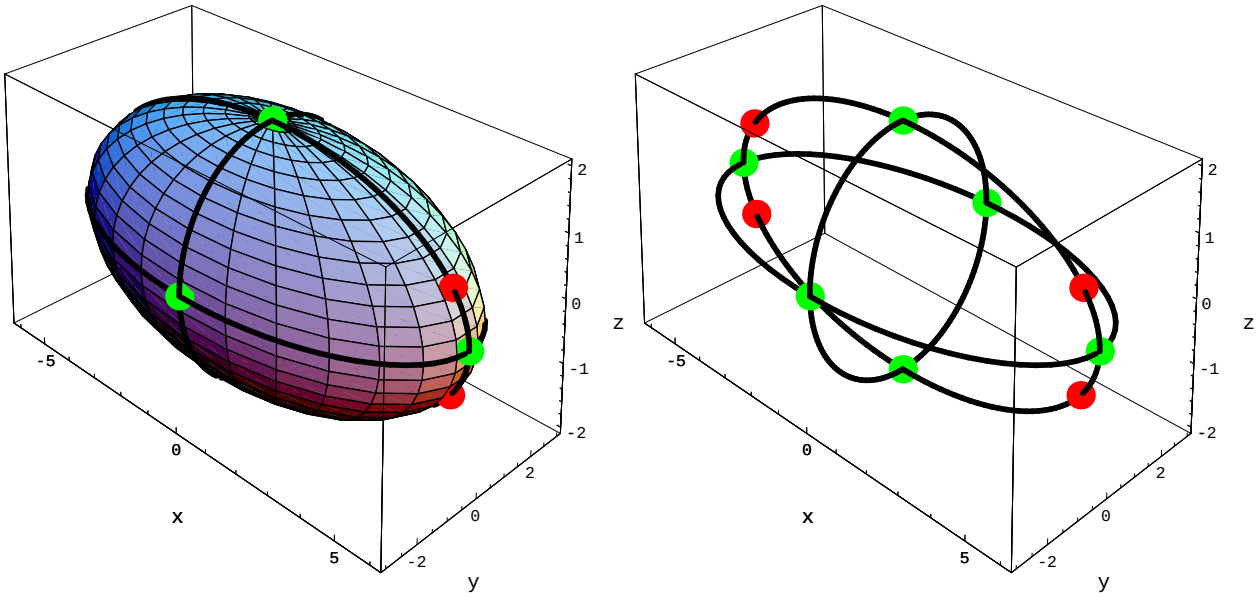

Figure 1: An ellipsiod with ridges and special points (see text).

2 Ellipsoid

Since 3D Medial Axis are hard to compute and visualize, the forcast for these tasks on the Symmetry Set is bad. In order to get at least the visualization as clear as possible, we investigate a simple shape that allows an exact computation, viz. an ellipsoid. Altough it is still very artificial, it is the first shape (next to the "degenerated´´ sphere) that gives a non-trivial Symmetry Set.

In (x, y, z) coordinates define a generic ellipsoid by

$$L(x, y, z) = \frac{x^2}{a^2} + \frac{y^2}{b^2} + \frac{z^2}{c^2} = 1,$$

with $a > b > c > 0$. The ellipsoid had its endpoints at $\pm(a, 0, 0)$, $\pm(0, b, 0)$, and $\pm(0, 0, c)$. An example with $(a, b, c) = (6, 3, 2)$ is given in Figure 1.

2.1 Ridge liness

The ridges of the ellipsoid occur at $x = 0$, $y = 0$, and $z = 0$. In Figure 1 they are visible as the curves. The intersect pairwise at the poles (bright blobs). Note that the apparently triple intersection is due to projection.

2.2 Umbilic points

The ellipsoid has four umbilic points (Porteous, geometric differentiation 267) [12] at $(\pm a\cos\phi, 0, c\sin\phi)$ with ϕ the solutions of $a^2\sin^2\phi + c^2\cos^2\phi = b^2$. In Figure 1 they are visible as the dark blobs.

2.3 Curvatures

Its Gaussian surface curvature K, Mean surface curvature, and the minimal and maximal curvatures follow directly from the previous section.

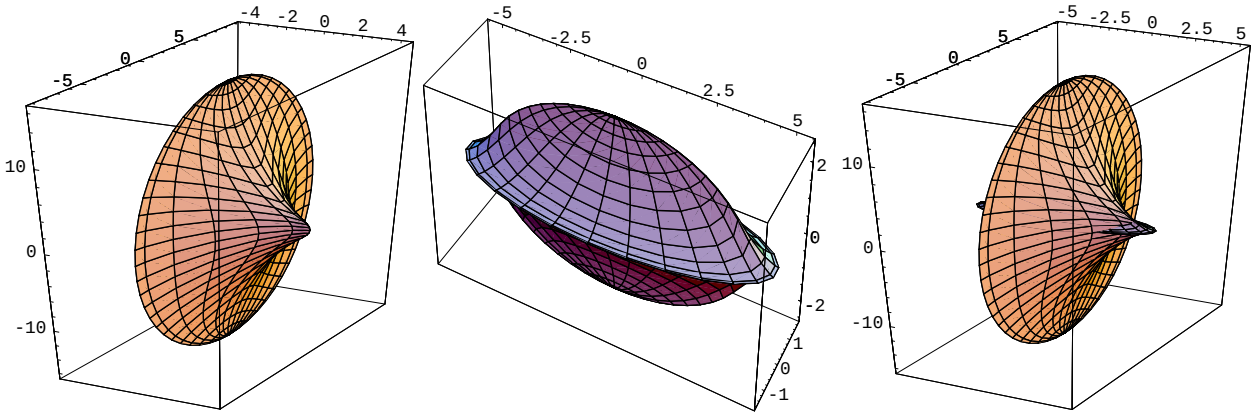

Figure 2: The evolutes for the ellipsoid. From left to right: depending on the maximal curvature, the minimal curvature, and both (intersecting) evolutes.

2.4 Evolutes

So to each point we can assign the points $\mathcal{S} + \mathcal{N}/\kappa_{min}$ and $\mathcal{S} + \mathcal{N}/\kappa_{max}$, defining two evolutes. They are shown in Figure 2. Note that the intersect, as shown in the right plot. The umbilic points lie on the intersection curves.

2.5 Implicit surface: (x, y, z) data

In the remainder, let $a = 6, b = 3, c = 2$. Then $\mathcal{N}(x, y, z) = (x, 4y, 9z)(x^2 + 16y^2 + 81z^2)^{-1/2}$, Locations of the SS are found at $(x, y, z) - r\mathcal{N}$. Since the shape is symmetric, the locations are at the $x = 0$, $y = 0$, and $z = 0$ planes.

Then for r the values $r_{x=0} = (x^2 + 16y^2 + 81z^2)^{1/2}$, $r_{y=0} = \frac{1}{4}(x^2 + 16y^2 + 81z^2)^{1/2}$, and $r_{z=0} = \frac{1}{9}(x^2 + 16y^2 + 81z^2)^{1/2}$ are found, with the SS planes $p_{x=0}$, $p_{y=0}$, and $p_{z=0}$. The planes are ellipses.

- **The first plane, $p_{x=0} = (0, -3y, -8z)$, is given by $(16y)^2 + (9z)^2 = (144)^2$, with its extremal positions $\pm(0, 9, 0)$ and $\pm(0, 0, 16)$**
- **The second one, $p_{y=0} = (3x/4, 0, -5z/4)$, is given by $(5x)^2 + (9z)^2 = (45/2)^2$, with its extremal positions $\pm(\frac{9}{2}, 0, 0)$ and $\pm(0, 0, \frac{5}{2})$**
- **The third one, $p_{z=0} = (8x/9, 5y/9, 0)$, is given by $(5x)^2 + (16y)^2 = (80/3)^2$, with its extremal positions $\pm(\frac{16}{3}, 0, 0)$ and $\pm(0, \frac{5}{3}, 0)$.**

This is visualized in Figure 3. The left image shows the planes. The bright point mark the positions of the pole-related points, while the dark points the umbilic related point represent. The lines are due to the ridges forming the boundaries of the planes - the A_3 curves- and the intersections of planes - A_1^2/A_1^2 lines. The origin is an $A_1^2/A_1^2/A_1^2$ point, while the intersetion with the A_3 curves result in A_1A_3 points. They are also shown in the middle image. The right image shows a close-up, where it can be seen that the umblic related points are indeed on the curves. The umbilic points are found to be at $\phi = \pm\arccos(\pm\frac{3}{8}\sqrt{6})$, at the points $(\pm\frac{9}{4}\sqrt{6}, 0, \pm\frac{1}{4}\sqrt{10})$.

In Figure 4 the close-up, the ellipsoid (opened), and the evolute (opend) are shown. One might be able to see that the evolutes intersect at the umbilic point. They also form the boundary of the Symmetry Set planes in the cusp-curves (just as the 2D Symmetry Set is bounded in the cusp-point of the evolute). At the umbilic point the two evolutes interchange their task in bounding the Symmetry Set plane that intersects the shape with its boundary. The other two planes have boundaries either completely inside (in this case the Medial Axis plane), or completely outside the shape.

In this simple case the pre-symmetry set can be computed exactly, and is given by the sets of points (x, y, z) combined with $(-x, y, z)$,$(x, -y, z)$, and $(x, y, -z)$.

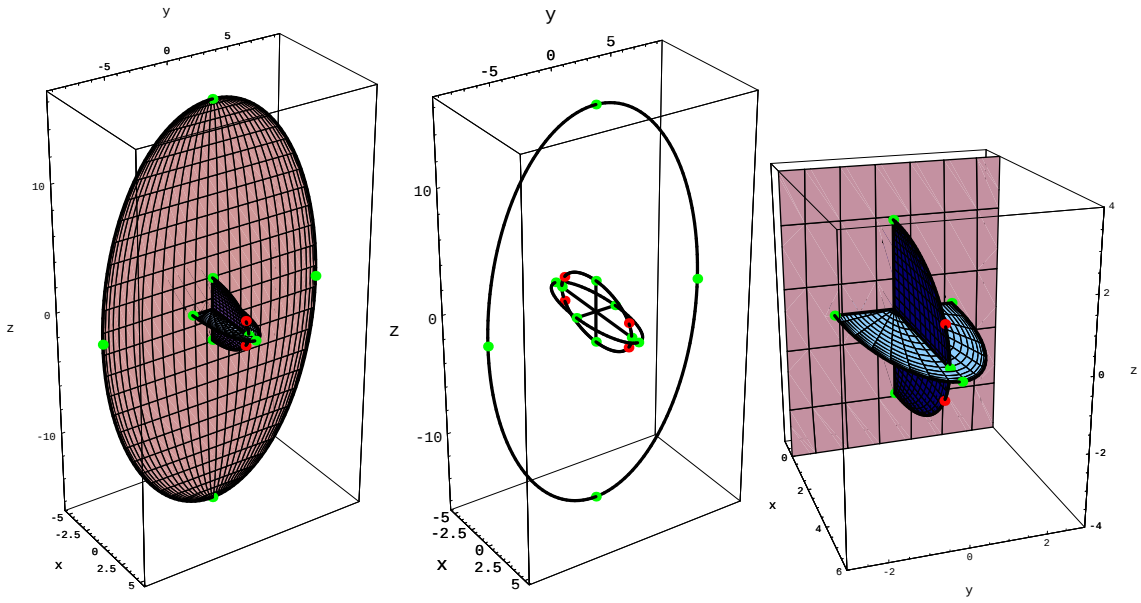

Figure 3: Left: symmetry set planes with special points and curves. Middle: The special curves and special points. Left: Close-up of the symmetry set planes with special points and curves.

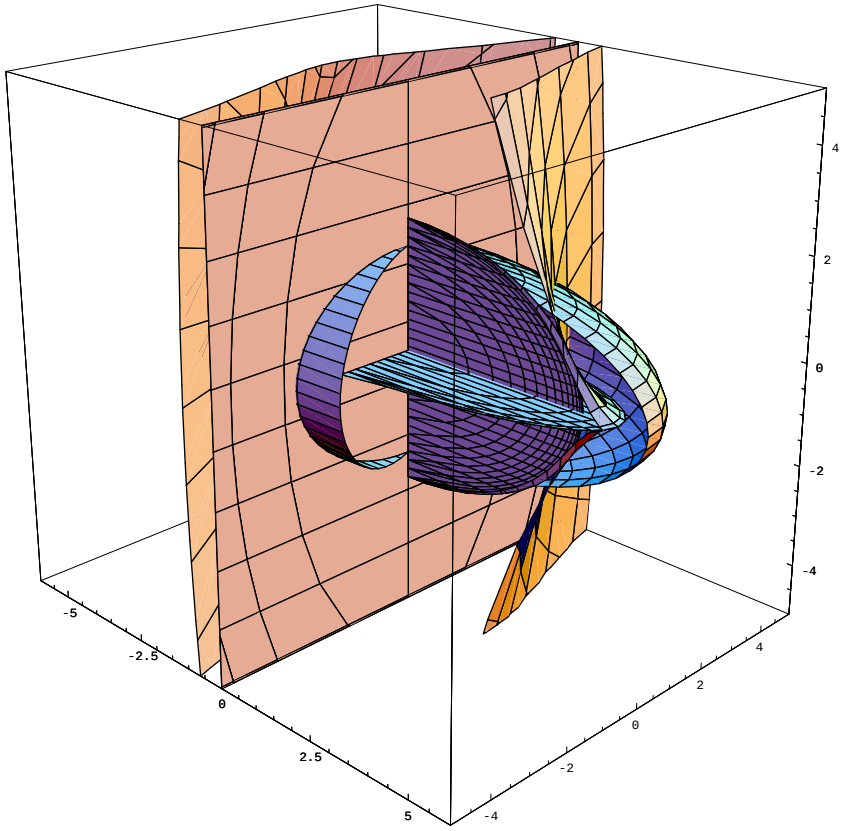

Figure 4: Complicated compilation of surfaces.

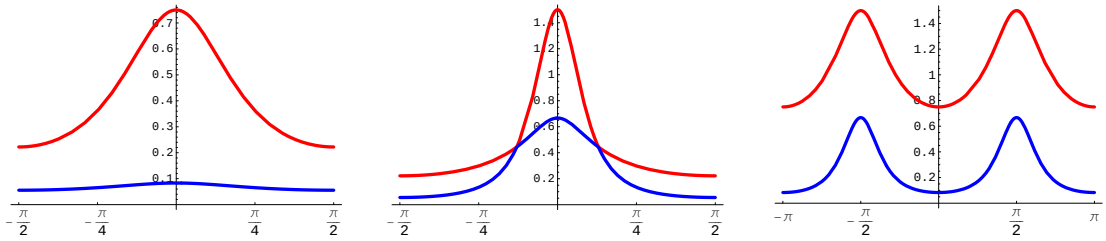

Figure 5: Curvatures along ridges. a) $x = 0$, b) $y = 0$, c) $z = 0$.

2.6 Parametrisation - s, t data

A parametrisation of L is given by

$$\begin{aligned} x &= 6 \sin s \cos t \\ y &= 3 \cos s \cos t \\ z &= 2 \sin t \end{aligned}$$

with $s \in [-\pi, \pi[$ and $t \in [-\frac{\pi}{2}, \frac{\pi}{2}[$. The extremal positions are obtained for

- $(s,t) = (s, -\frac{\pi}{2})$**, i.e.** $(x,y,z) = (0,0,-2)$**,**
- $(s,t) = (s, \frac{\pi}{2})$**, i.e.** $(x,y,z) = (0,0,2)$**,**
- $(s,t) = (0,0)$**, i.e.** $(x,y,z) = (0,3,0)$**,**
- $(s,t) = (\pi,0)$**, i.e.** $(x,y,z) = (0,-3,0)$**,**
- $(s,t) = (\frac{\pi}{2},0)$**, i.e.** $(x,y,z) = (6,0,0)$**, and**
- $(s,t) = (-\frac{\pi}{2},0)$**, i.e.** $(x,y,z) = (-6,0,0)$**.**

Note that for $t = -\frac{\pi}{2}, \frac{\pi}{2}[$ the two poles are obtained. There all s values coincide. Ridge lines - A_3 curves of the SS - are found on the boundary of each ellipse. The symmetry set planes are given by $p_{x=0} = (0, -3y, -8z)$, so $(x,y,z) = (0, -9\cos s \cos t, -16 \sin t)$, $p_{y=0} = (3x/4, 0, -5z/4)$, so $(x,y,z) = (\frac{9}{2} \sin s \cos t, 0, -\frac{5}{2} \sin t)$, and $p_{z=0} = (8x/9, 5y/9, 0)$, so $(x,y,z) = (\frac{16}{3} \sin s \cos t, \frac{5}{3} \cos s \cos t, 0)$.

The curvatures along the ridges are shown in Figure 5. The intersection of the two curvatures in the middle graph is due to the umbilic points. The curvatures coincide for $(s,t) = (\pm\frac{1}{2}\pi, \pm \arccos(\pm\frac{3}{8}\sqrt{6}))$. These D_4^+ points are on the boundary of $p_{y=0}$. They do not affect the ellipse, although the minimal curvature (bounding the Symmetry Set) has a non-differential point there.

2.7 Pre-symmetry set surfaces

For the presymmetry set we find the sets

- $(s,t,-s,t)$ **(for $(x,y,z) = (-x,y,z)$),**
- $(s,t,\|\pi - s\|_\pi, t)$ **(for $(x,y,z) = (x,-y,z)$), and**
- $(s,t,s,-t)$ **(for $(x,y,z) = (x,y,-z)$).**

The axis of symmetry in the pre-symmetry set are, respectively,

- $s = 0, \pi$ **i.e.** $(x,y,z) = (0, \pm 3\cos t, 2 \sin t)$**, the ridge in the $x = 0$ plane,**
- $s = \pm\pi/2$ **i.e.** $(x,y,z) = (\pm 6 \cos t, 0, 2 \sin t)$**, the ridge in the $y = 0$ plane, and**
- $t = 0$ **i.e.** $(x,y,z) = (6 \sin s, 3 \cos s, 0)$**, the ridge in the $z = 0$ plane.**

Therefore the ridge lines in the presymmetry set are formed by the curves $(0,t,0,t)$, (π,t,π,t), $(\pi/2,t,\pi/2,t)$, $(-\pi/2,t,-\pi/2,t)$, and $(s,0,s,0)$. Intersections take place at

- **$(s,t,-s,t) = (s,t,s,-t)$, so $s = 0,\pi$ and $t = 0$ due to boundary conditions of s and t. Therefore intersections occur at $(s,t) = (0,0)$, i.e. $(x,y,t) = (0,3,0)$, and $(s,t) = (\pi,0)$, i.e. $(x,y,t) = (0,-3,0)$. This implies that they occur at the extremal points on the y-axis. This intersection implies $(-x,y,z) = (x,y,-z)$, so $(x,y,z) = (0,y,z]$ is expected, with $y = \pm 3$: the intersection of the two ridges in the $x = 0$ and $z = 0$ planes.**
- **$(s,t,s,-t) = (s,t,\|\pi - s\|_\pi,t)$so $s = \pm\pi/2$ and $t = 0$. Then $(s,t) = (-\pi/2,0)$, i.e. $(x,y,t) = (-6,0,0)$, and $(s,t) = (\pi/2,0)$, i.e. $(x,y,t) = (6,0,0)$. This implies that they occur at the extremal points on the x-axis.**
- **$(s,t,-s,t) = (s,t,\|\pi - s\|_\pi,t)$, so $t = \pm\pi/2$. Then $(s,t) = (s,-\pi/2)$, i.e. $(x,y,t) = (0,0,-2)$, and $(s,t) = (s,\pi/2)$, i.e. $(x,y,t) = (0,0,2)$. This implies that they occur at the extremal points on the z-axis, the poles.**

Therefore, intersections of the pre-symmetry set surfaces occur at the extremal values of the ellipsiod.

3 Computation

In the following sections we present three different ways to compute the 3D symmetry set of the ellipsoid. The 3D symmetry set is defined similar to the 2D case: the closure of centers of spheres tangent to the shape at at least two points. The radius r and the center of the sphere are given by

$$p_i - rN_i = p_j \pm rN_j \tag{1}$$

3.1 Exact computation

For the exact computation, we take the parametrised ellipsoid and get a set of datapoints by choosing $s = \frac{\pi}{20} + i\frac{\pi}{10}$, $i = 0,1,\ldots,19$, and $t = -\frac{\pi}{2} + \frac{\pi}{40} + j\frac{\pi}{20}$, $j = 0,1,\ldots,19$. So there are 20 x 20 datapoints, see Figure 6a. Note that the poles and ridges are not taken into the parametrisation.

Next, the pre-SS is *constructed* by choosing the sets $(s,t,-s,t)$, $(s,t,\|\pi - s\|_\pi,t)$, and $(s,t,s,-t)$. The corrsponding SS is derived from the 3D extension of the 2D algorithm "pre-SS to SS", presented in deliverable 10. It solves equation 1 exactly by construction of the pre-SS.

The results are shown in Figure 6b. The separate planes are visualized in Figure 7.

As a check of the correctness of the solution, we verify that the minimum absolute value of each triple (x,y,z) that is found as an SS point, is "close enough" to zero: note that the SS points form filled ellipses in the $x = 0$, $y = 0$, or $z = 0$ planes. This graph is shown in Figure 8. It is within machine precision, $O(10^{-16})$. Note that 600 points (200 in each plane) are found. The algorithm generates 3 x 20 x 20 = 1200 points, but half of them occur double due to symmetry.

3.2 Extention of the 2D zero-crossings algorithm

If the pre-SS needs to be computed from the data points and their normal vectors, similar equations hold as in the 2D case for the zero-crossings algorithm if the shape is (s,t)-parametrized and p_1 is short notation for $p(s_1,t_1)$:

$$\begin{array}{rcl}(p_1 - p_2).(N_i \pm N_j) & = & 0 \\ (p_1 - p_2).(N_i \times N_j) & = & 0\end{array} \tag{2}$$

The second constraint is new in 3D and rises from the fact that the line $(N_i \times N_j)$ is the intersectionof the two normal planes. This line is given by $(N_{y1}N_{z2} - N_{y2}N_{z1}, -N_{x1}N_{z2} + N_{x2}N_{z1}, N_{x1}N_{y2} - N_{x2}N_{y1})$.

As in the 2D case, the Anti Symmetry Set points should be removed from this set. These points satisfy the fact that there tangent planes are parallel. Equivalently, the normals are aligned. Consequently, the normal at the first point is perpendicular to the tangent plane at the second plane. This plane is computed as follows. Let $v_1 =$

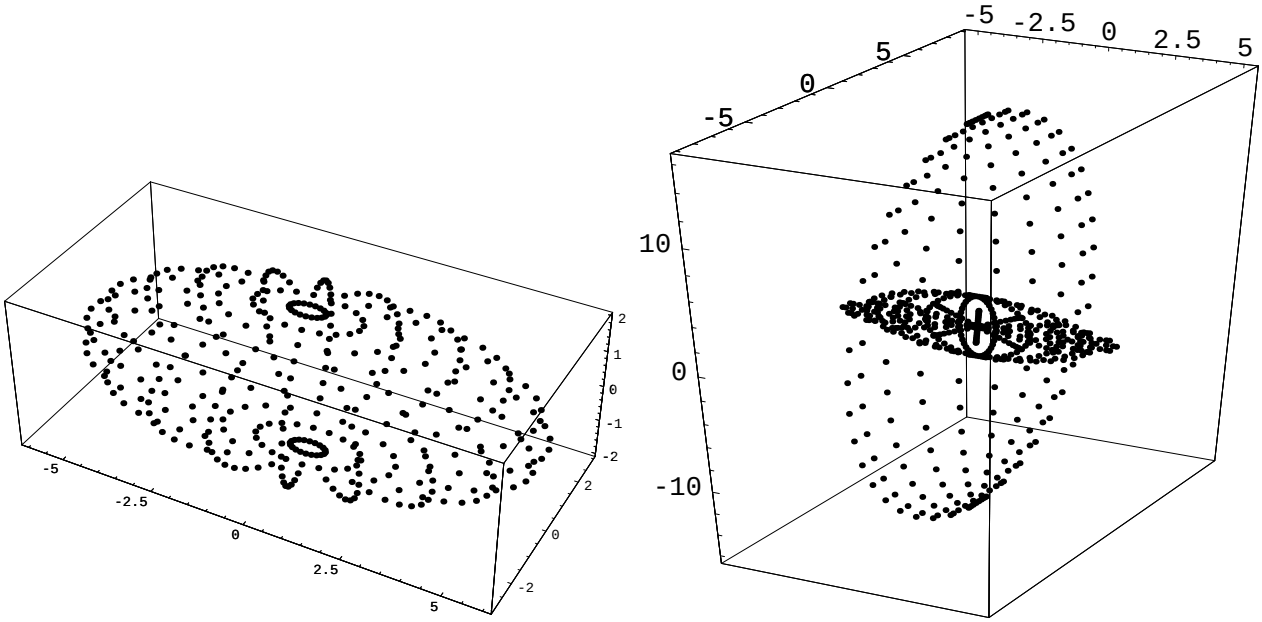

Figure 6: a) Selected points. b) Symmetry Set.

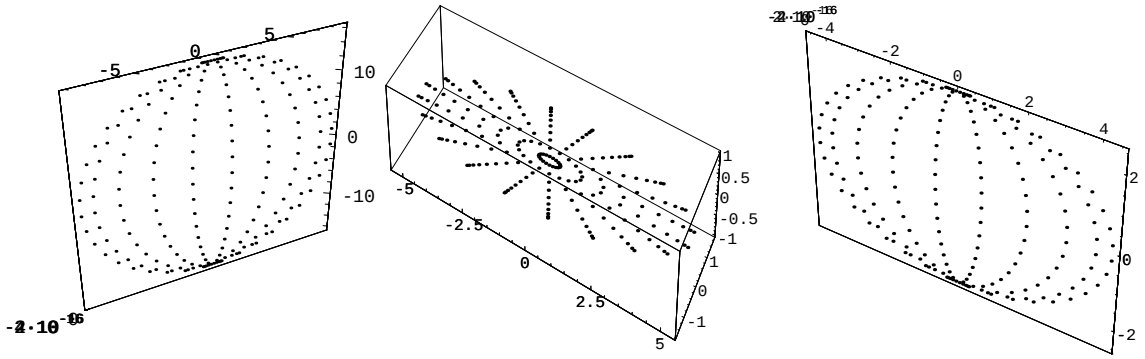

Figure 7: 3 distinct planes of the Symmetry Set.

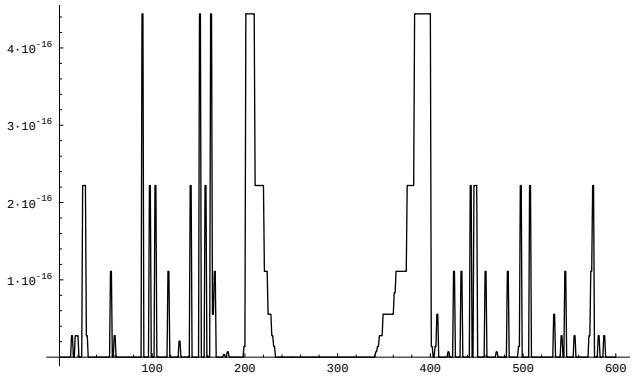

Figure 8: Minimum absolute value of each SS triple (x, y, z), ideally equal to zero.

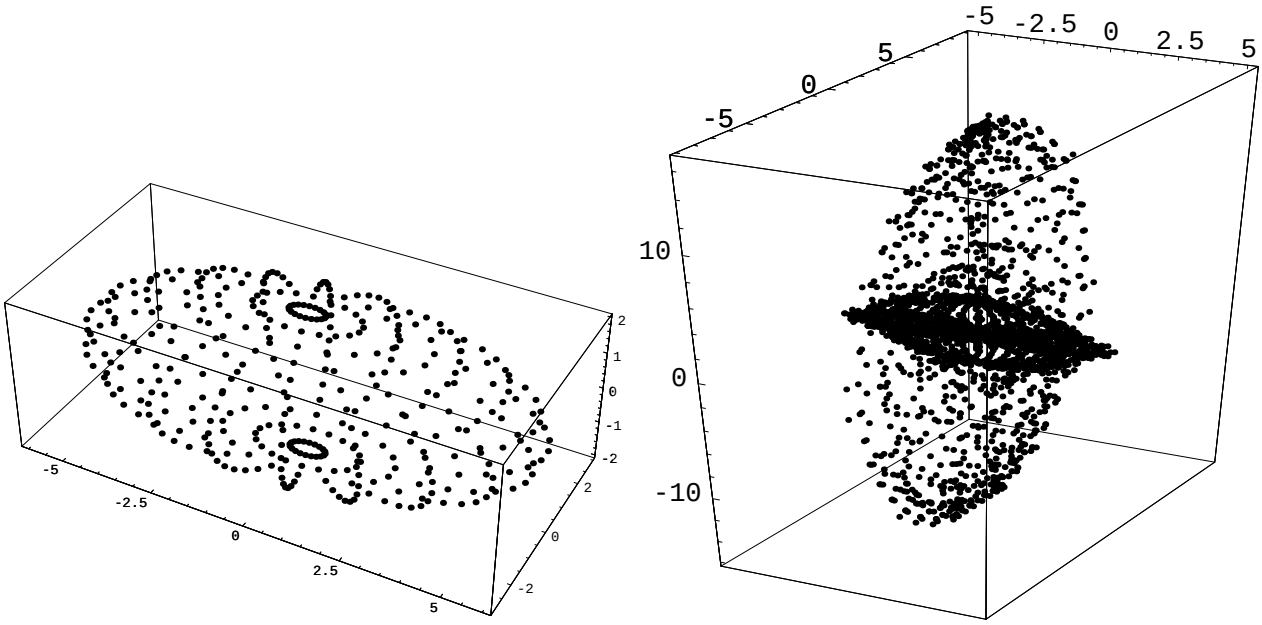

Figure 9: a) Selected points. b) Symmetry Set.

$N_1 = (a, b, c)$**. Then two vectors are sought that satisfy** $v_1.v_2 = 0$**,** $v_1.v_3 = 0$**, and** $v_2.v_3 = 0$**. One combination satisfying these constraints is the set** $v_2 = (-2bc, ac, ab)$ **and** $v_3 = (ab^2 - ac^2, -a^2b - 2bc^2, a^2c + 2b^2c)$**.**

So the ASS is found as the intersection of the solutions of

$$\begin{array}{c}(N_{x1}, N_{y1}, N_{z1}).(2N_{y2}N_{z2}, N_{x2}N_{z2}, N_{x2}N_{y2}) = 0 \\ (N_{x1}, N_{y1}, N_{z1}).(N_{x2}N_{y2}^2 - N_{x2}N_{z2}^2, -N_{x2}^2N_{y2} - 2N_{y2}N_{z2}^2, N_{x2}^2N_{z2} + 2N_{y2}^2N_{z2}) = 0\end{array} \tag{3}$$

Note that the pre-SS space is a 4D space. The zero-crossings are obtained by taking changes in the signs of the equations above in all four directions.

3.2.1 Calculation of the pre-SS and SS

To compute the pre-SS, one should be careful. If the data is constructed as in the previous section, one enters exact solutions of the positions of zero-crossings. This is non-generic in general, and the algorithm, detecting only full signchanges, will fail to find these points. So additional infinitesimal noise should be added to generate a generic parametrized pointcloud. Noise is taken in the order of $O(10^{-5})$ **and affects both the positions - so points may be slightly off-ellipse, and normals - so they are not calculated at the right position and do not have exactly unit length. The pointcloud, Figure 9a,looks similar to the unpertured cloud.**

In this case with 400 data points computational time is reaching the limits of being acceptable. It takes the algorithm 8.4 seconds to find 24216 points fot the first zerocrossing, and 11.4 seconds to find 55556 points for the second zerocrossing, yielding 8210 points on the intersection. Next, it takes 7.4 seconds to find 73359 points fot the first ASS zerocrossing, and 11.2 seconds to find 63226 points fot the second ASS zerocrossing, yielding 30104 ASS points as intersection. The complement of both intersection results gives 5438 SS-solutions, but since the pre-SS is symmetric, in total 2719 SS-points are found. The resulting symmety set is shown in Figure 9b.

Next, the points in the three planes shown in Figure 10. This is a view of the SS along each of the three axes, while the plot area is restricted to $(-.1, .1)$**.**

As one can see there are some outlyers. This is verified by the minimum absolute value of each triple (x, y, z) **that is found as an SS point. These minimal values-graph is shown in Figure 11. The left image indicates some symmetry, that is indeed present due to the algorithm**

The largest value is caused by the point $(-2.16, -1.62, -2.74)$**. It resembles to points at** $p_1 = (-4.94, 1.26, .7653)$ **and** $p_2 = (-3.92, 1.96, 7654)$**. Apparently, their** z **values are close. We have** $\|p_1 - p_2\| = 1.24$**,** $\|N_1 - N_2\| = 0.257$**,**

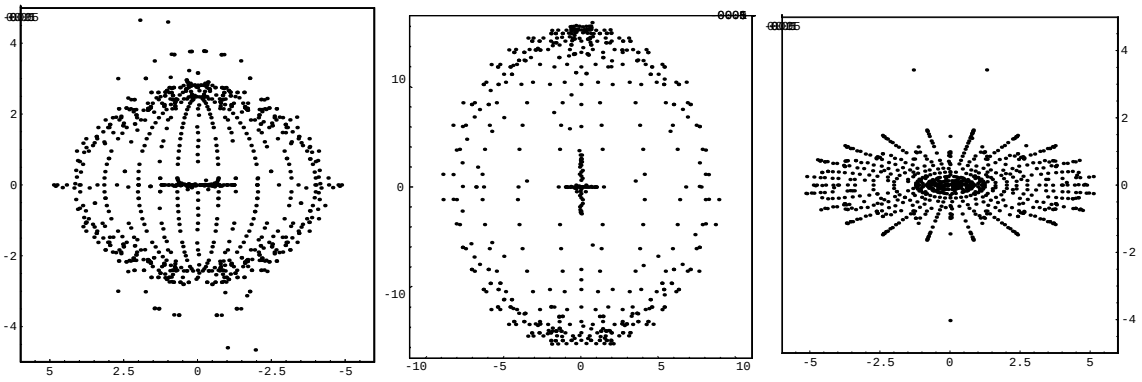

Figure 10: 3 distinct planes of the Symmetry Set.

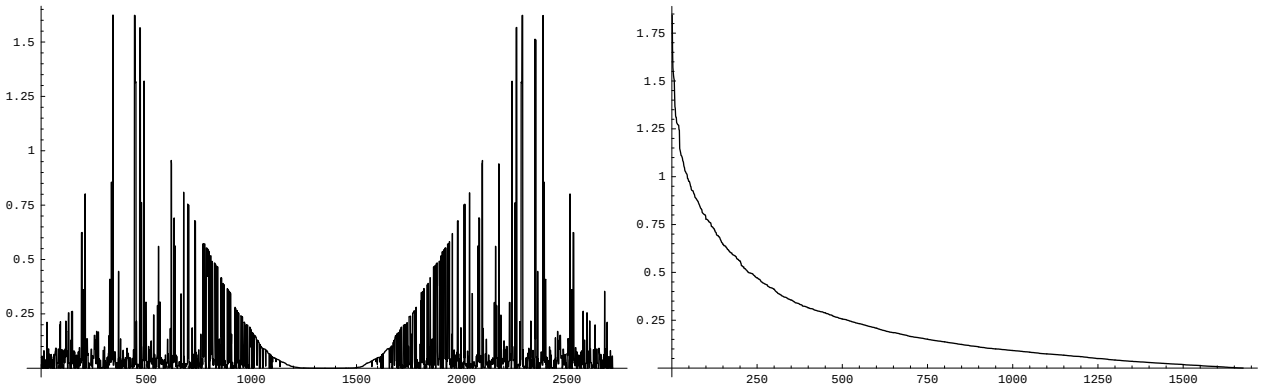

Figure 11: Minimum absolute value (unsorted and sorted) of each SS triple (x, y, z), ideally equal to zero.

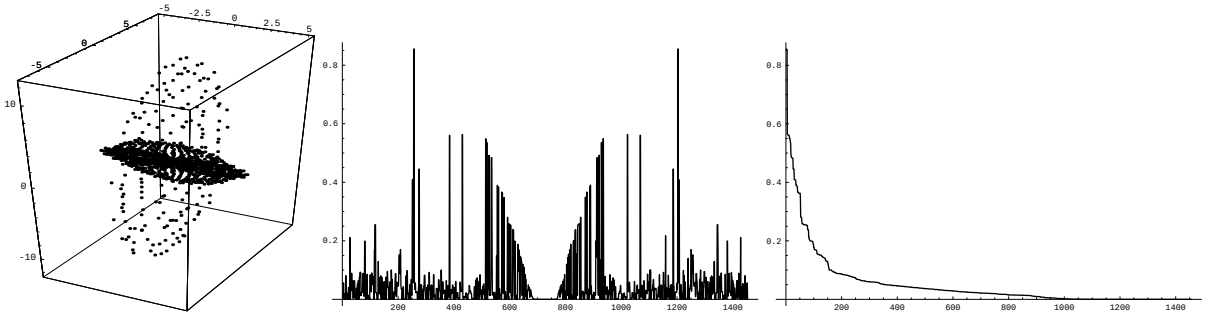

Figure 12: min norm constraint.

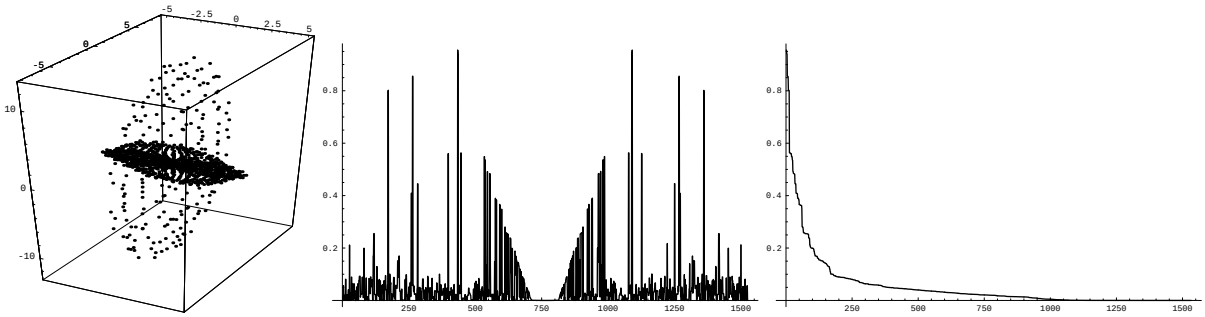

Figure 13: max norm constraint.

$\|N_1 + N_2\| = 1.98$**, $\|N_1 \times N_2\| = .255$. For the two zerocrossing values we find values $(p_1 - p_2).(N_1 + N_2) = .02$ and $(p_1 - p_2).(N_1 \times N_2) = .13$, normalized they are $.007$ and $.43$, respectively. Apparently they are found of zero crossings, but due to the relatively flatness of the shape their positions cause a large error in the position.**

3.2.2 On outlyers

Lets look into ASS points more detailed. Consider the tangent circle for a point $p_1 = (x, y, z)$ with corresponding normal $N_1 = (N_x, N_y, N_z)$. We have as SS point, say, $p_2 = (-x, y, z)$ with corresponding normal $N_2 = (-N_x, N_y, N_z)$, and as an ASS point, say, $p_3 = (-x, -y, z)$ with corresponding normal $N_3 = (-N_x, -N_y, N_z)$.

Now $p_1 - p_2 = (2x, 0, 0)$, $N_1 - N_2 = (2N_x, 0, 0)$, $N_1 + N_2 = (0, 2N_y, 2N_z)$, $N_1 \times N_2 = (0, -2N_xN_y, 2N_yN_x)$. So $(p_1 - p_2).(N_1 + N_2) = 0$ and $(p_1 - p_2).(N_1 \times N_2) = 0$.

Als $p_1 - p_3 = (2x, 2y, 0)$, $N_1 - N_3 = (2N_x, 2N_y, 0)$, $N_1 + N_3 = (0, 0, 2N_z)$, $N_1 \times N_3 = (2N_yN_z, -2N_xN_z, 0)$. So $(p_1 - p_3).(N_1 + N_3) = 0$ and $(p_1 - p_3).(N_1 \times N_3) = 4N_z(xN_y - yN_x)$ which may become (close to) zero for certain combinations of points, especially when two points are nearby. If this is the case, the two normals are almost pointing into the same direction and the norm of their sum is close to 2, and subtracting yields almost 0. So as an extra check one can remove these point combinations.

So, experiment 1: require that $\|N_1 - N_2\| > \epsilon \geq 0$. For $\epsilon = .25$ 1926 SS points are left. However, the point mentioned above is still part of the SS. For $\epsilon = .5$ 2912 SS points are left. The maximal minum values are significantly lower. See Figure 12.

Experiment 2: require that $\|N_1 + N_2\| < \epsilon \leq 2$. For $\epsilon = 1.98$ 1906 SS points are left. Also in this case, the point mentioned above is still part of the SS. For $\epsilon = 1.95$ 3066 SS points are left. The maximal minum values are again significantly lower. See Figure 13.

Apparently subtracting is less sensitive. Furthermore, setting this norm seems to affect the large SS-ellipse. This makes sense, since it depends on the parts of the shape that are most flat, requires longest radii and have (thus) normals that are close to each other.

Another constraint may be requiring that the normalised inner product values of the vectors found as zerocrossings, is small. Set it to $.2$ for both, in combination with $\|N_1 - N_2\| > .5$, gives 994 points with

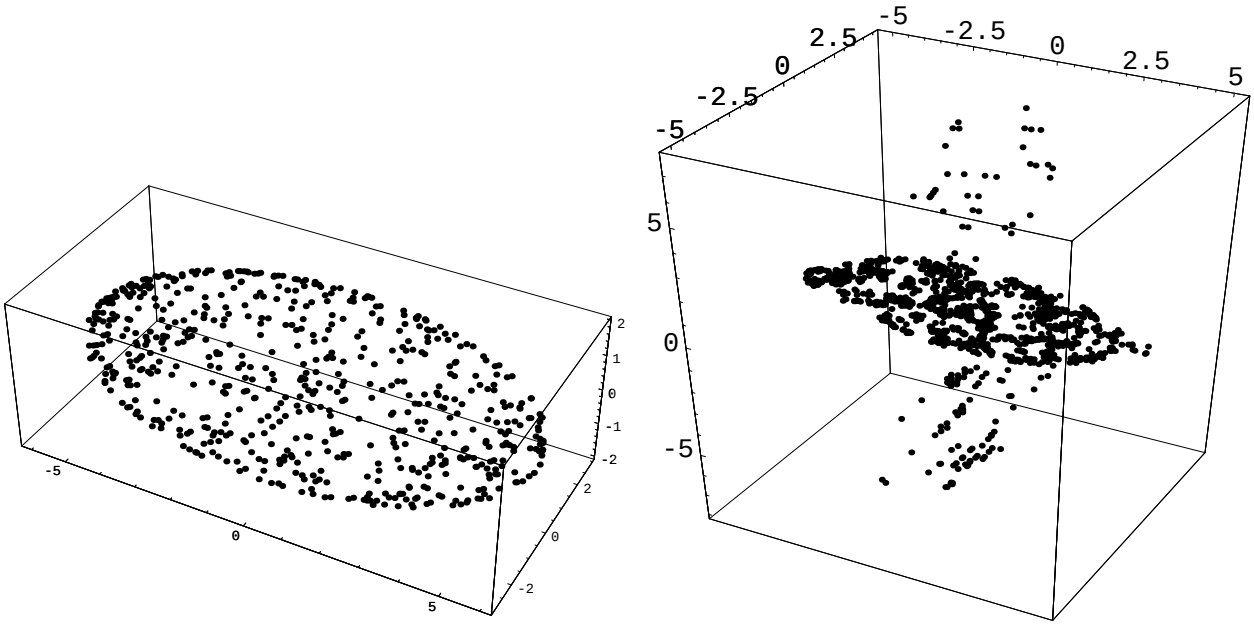

Figure 14: a) Randomly selected points. b) Symmetry Set.

maximum minimal error value $.55$. This opens possibilities to the next appraoch.

3.3 Symmetry Sets from Point Cloud

Apparently, the parametrisation causes problems, especially at the north and south poles, but also at points nearby. To overcome these problems, extra constraints can be added. What one does in that case, is not looking for zero crossings explicitly, but pairs of points that are close enough to be considered as zero crossings. Now zero crossings require a parameterization, but the "close enough appraoch´´ can be considered as parameterless.

It is therefore worth the effort to investigate what these constraints would do on a random point set. That is, given an arbitrary set of points $p_i$on the ellips with unit normals N_i, select each combination satisfying

$$\begin{array}{rcl} (p_1 - p_2).(N_1 + N_2) & < & \delta_1 \\ (p_1 - p_2).(N_1 \times N_2) & < & \delta_2 \\ \|N_1 - N_2\| & > & \epsilon \end{array} \tag{4}$$

and define this set as the Symmetry Set.

This appraoch has been taken in the following. A random point set on the ellipsoid is taken in the (x, y, z) space, see Figure 14. A selection in the (s, t) space yields a similar cloud, although more points are close to the north and south poles. Since the normal vectors are known by definition, regularization is not needed and the Symmetry Set can be computed directly. With 1000 points, 10191 Symmetry Set points are found in 150 seconds. Limiting to 500 points, 2573 points are found in 37 seconds. For the latter we set $\delta_1 = .1$, $\delta_2 = .75$, and $\epsilon = 1.95$, yielding 1599 points.

The individual planes of the outcome are shown in Figure 15. One can see that the large plane is least detailed, as expected.

The deviation from the planes is in the order of the previous calculations, see Figure 16. Off course, more tuning of the parameters δ_1, δ_2, and ϵ may inprove the performance.

Figure 15: 3 distinct planes of the Symmetry Set.

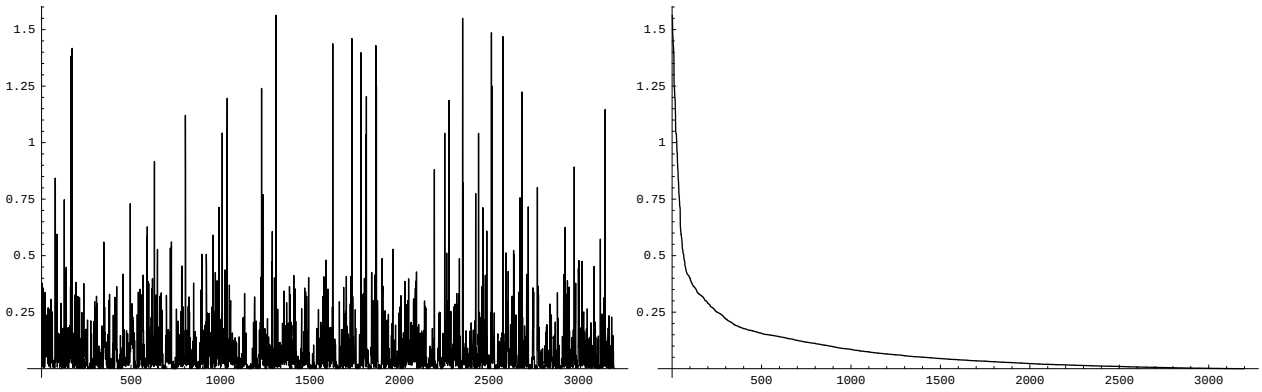

Figure 16: Minimum absolute value of each SS triple - random point cloud.

4 Conclusions and perspectives

For shapes in 3D, the Symmetry Set can be computed using a simple extension of the approach taken in the 2D case. With the same argumentation as for the 2D case, PDE methods are not available for computation and the geometric appraoch must be taken. Although this isan almost trivial extension, numerical problems arise earlier than in the 2D case. Since the algorithms imply computation of the pre-Symmetry Set, the complexity of the algorithm prohibits large data sets. A refinement of the shape in adding more data points is therefore not possible.

The zero crossings method used requires a parameterisation. Since additional parameters / thresholds are needed to avoid numerical instabilities, the parameterization may as well be ignored and the method works on unordered point clouds. In the example given the normal vectors were known a priori, but if they need to be estimated by means of some kind of regularisation, (large) errors may be introduced. This needs more experiments.

Next, the visualization of the Symmetry Set in 3D is hard. It cannot be avoided by using the pre-Symmetry Set, since this set lives in an 4D space, albeit that the set itself contains only 2D manifolds. The use of this set and some of the mathematical properties are to be described in deliverable 22 on alternative descriptions of Symmetry Sets.

For representational purposes, the Gauss diagrams may be useful. A 2D version of these diagrams is described in chapter 4. In 3D they are formed by spheres - or worse, manifolds with holes, depending on the original shape.

References

[1] **J. W. Bruce, P. J. Giblin, and C. Gibson. Symmetry sets. *Proceedings of the Royal Society of Edinburgh*, 101(A):163–186, 1985.**

[2] **P. J. Giblin and B. B. Kimia. A formal classification of the 3D medial axis points and their local geometry. In *IEEE Conference on Computer Vision and Pattern Recognition, 2000*, pages 566–573, 2000.**

[3] **P. J. Giblin and B. B. Kimia. Transitions of the 3D medial axis under a one-parameter family of deformations. In *Proceedings of the 7th European Conference on Computer Vision (2002)*, pages 718–734, 2002. LNCS 2351.**

[4] **P. J. Giblin and B. B. Kimia. A formal classification of the 3D medial axis points and their local geometry. *IEEE Transactions on Pattern Analysis and Machine Intelligence*, 26(2):238–251, 2004.**

[5] **M. Hisada, A. G. Belyaev, and T. L. Kunii. Towards a singularity-based shape language: ridges, ravines, and skeletons for polygonal surfaces. *Soft Computing*, 7(1):45–52, 2002.**

[6] **J. J. Koenderink. *Solid Shape*. MIT Press, Cambridge, Massachusetts, 1990.**

[7] **F. Leymarie. *3D Shape Representation via Shock Flows*. PhD thesis, Division of Enginering., Brown University, Providence, RI, 02912, 2003.**

[8] **F. Leymarie and B.B. Kimia. The shock scaffold for representing 3D shapes. In *Proceedings International Workshop on Visual Form*, volume 2059, pages 216–228, 2001. LNCS 2059.**

[9] **F. Leymarie and B.B. Kimia. Symmetry-based representation of 3D data. In *Proceedings IEEE International Conference on Image Processing*, pages 581–584, 2001.**

[10] **F. Leymarie and B.B. Kimia. Computation of the shock scaffold for unorganized point clouds in 3D. In *Proceedings IEEE Computer Society Conference on Computer Vision and Pattern Recognition (CVPR'03)*, volume 1, pages 821–827, 2003.**

[11] **F. Leymarie, B.B. Kimia, and P.J. Giblin. Towards surface regularization via medial axis transitions. In *Proceedings IEEE International Conference on Pattern Recognition (ICPR'04)*, volume 3, pages 123–126, 2004.**

[12] **Ian Porteous. *Geometric Differentiation - for the intelligence of curves and surfaces*. Cambridge University Press, Cambridge, UK, 1994. 301 pages.**